

# Some computational results for $\mathbf{P}_1 - P_1$ and $\mathbf{P}_2 - P_1$ Trace FEM for the surface Stokes problem

Alexander Zhiliakov\*

April 20, 2019

## Contents

<b>1</b>	<b>Inf-sup stability: generalized pressure Schur complement eigenvalues</b>	<b>1</b>
1.1	Bilinear forms and matrices . . . . .	1
1.2	Solution description . . . . .	2
1.3	Numerical results: dependency of the spectrum on the mesh size . . . . .	3
1.4	Numerical results: sensitivity of the spectrum to levelset shifts . . . . .	6
<b>2</b>	<b>Convergence results</b>	<b>8</b>
2.1	$\mathbf{P}_1 - P_1$ Trace FEM . . . . .	8
2.2	$\mathbf{P}_2 - P_1$ Trace FEM . . . . .	10
<b>3</b>	<b>Notes on DROPS implementation</b>	<b>11</b>
3.1	Notations . . . . .	11
3.2	Approximation of integrands involving $\mathbf{n}_\Gamma$ . . . . .	11
3.3	Quadrature rules for $\int_\Gamma$ and $\int_{\Omega_\Gamma^h}$ . . . . .	13
3.4	Summary on the matrix assembly . . . . .	15
3.5	Using exact normals in integrands of $\int_{\Gamma^{2 \rightarrow 1}_{h/m}}$ (updated summary) . . . . .	15
3.6	Quadrature rules for the error computation . . . . .	18

## 1 Inf-sup stability: generalized pressure Schur complement eigenvalues

### 1.1 Bilinear forms and matrices

We set  $n_{\mathbf{A}}$  to be the number of velocity d.o.f. and  $n_{\mathbf{S}}$  to be the number of pressure d.o.f. Vector stiffness, divergence, pressure mass, normal stabilization, and full stabilization matrices resulting from Trace FEM

---

\*Department of Mathematics, University of Houston, Houston, Texas 77204 (alex@math.uh.edu).

discretization of the surface Stokes problem [1] are defined via

$$\begin{aligned}
\langle \mathbf{A} \vec{\mathbf{u}}, \vec{\mathbf{v}} \rangle &\approx \int_{\Gamma} (E_s(\mathbf{u}) : E_s(\mathbf{v}) + \mathbf{u} \cdot \mathbf{v} + \tau (\mathbf{u} \cdot \mathbf{n}) (\mathbf{v} \cdot \mathbf{n})) \, ds + \rho_u \int_{\Omega_h^\Gamma} \frac{\partial \mathbf{u}}{\partial \mathbf{n}} \cdot \frac{\partial \mathbf{v}}{\partial \mathbf{n}} \, d\mathbf{x}, \quad \mathbf{A} \in \mathbb{R}^{n_{\mathbf{A}} \times n_{\mathbf{A}}}, \\
\langle \mathbf{B} \vec{\mathbf{u}}, \vec{\mathbf{q}} \rangle &\approx - \int_{\Gamma} q \, \text{div}_{\Gamma} \mathbf{u} \, ds, \quad \mathbf{B} \in \mathbb{R}^{n_{\mathbf{S}} \times n_{\mathbf{A}}}, \\
\langle \mathbf{M}_0 \vec{\mathbf{p}}, \vec{\mathbf{q}} \rangle &\approx \int_{\Gamma} p q \, ds, \quad \mathbf{M}_0 \in \mathbb{R}^{n_{\mathbf{S}} \times n_{\mathbf{S}}}, \\
\langle \mathbf{C}_n \vec{\mathbf{p}}, \vec{\mathbf{q}} \rangle &\approx \rho_p \int_{\Omega_h^\Gamma} \frac{\partial p}{\partial \mathbf{n}} \frac{\partial q}{\partial \mathbf{n}} \, d\mathbf{x}, \quad \mathbf{C}_n \in \mathbb{R}^{n_{\mathbf{S}} \times n_{\mathbf{S}}}, \\
\langle \mathbf{C}_{\text{full}} \vec{\mathbf{p}}, \vec{\mathbf{q}} \rangle &\approx \rho_p \int_{\Omega_h^\Gamma} \nabla p \cdot \nabla q \, d\mathbf{x}, \quad \mathbf{C}_{\text{full}} \in \mathbb{R}^{n_{\mathbf{S}} \times n_{\mathbf{S}}},
\end{aligned} \tag{1}$$

respectively. We use notations as in [1], in particular,  $\Omega_h^\Gamma$  is the domain consisting of tetrahedra cut by  $\Gamma$ . Here  $\vec{\mathbf{u}}$  denotes a vector of d.o.f. corresponding to a FE interpolant  $\mathbf{u}$  (analogously for  $\vec{\mathbf{p}}$  and  $p$ ). See (16) and (17) for the computational details. Mesh-dependent parameters are set as

$$\tau = h^{-2}, \quad \rho_u = \rho_p = h, \tag{2}$$

and  $h$  is the typical mesh size for tetrahedra from  $\Omega_h^\Gamma$ .  $\Gamma$  is chosen either as the unit sphere or torus,  $\Gamma = \Gamma_{\text{sph}}$  or  $\Gamma = \Gamma_{\text{tor}}$  (see Figure 1).

We also define matrices

$$\mathbf{C}_0 := \mathbf{0}, \quad \mathbf{M}_n := \mathbf{M}_0 + \mathbf{C}_n, \quad \mathbf{M}_{\text{full}} := \mathbf{M}_0 + \mathbf{C}_{\text{full}}. \tag{3}$$

We are interested in (generalized) extreme eigenvalues of the pressure Schur complement matrices

$$\mathbf{S}_0 := \mathbf{B} \mathbf{A}^{-1} \mathbf{B}^T, \quad \mathbf{S}_n := \mathbf{S}_0 + \mathbf{C}_n, \quad \mathbf{S}_{\text{full}} := \mathbf{S}_0 + \mathbf{C}_{\text{full}}, \tag{4}$$

i.e. in solving

$$\mathbf{S}_\star \mathbf{x} = \lambda \mathbf{M}_\star \mathbf{x}, \tag{5}$$

where “ $\star$ ” stands for “0,” “ $n$ ,” or “full.” We denote by  $0 = \lambda_1 < \lambda_2 \leq \dots \leq \lambda_{n_{\mathbf{S}}} = O(1)$  the spectrum of (5).

## 1.2 Solution description

Computing  $\mathbf{A}^{-1}$  in (4) becomes troublesome already for  $h = 5.21 \times 10^{-2}$  ( $n_{\mathbf{A}} = 32736$  for  $\mathbf{u} \in \mathbf{P}_1$  FE space): although  $\mathbf{A}$  is sparse,  $\mathbf{A}^{-1}$  is dense and consumes 8.5+ GB in double-precision arithmetic. A quick research showed that **Mathematica** has no built-in matrix-free eigenvalue routines. **Intel MKL**’s FEAST algorithm for computing (generalized) eigenvalues in an interval is suitable for matrix-free implementations; however, it requires some expensive operations to be implemented (e.g. matrix-matrix multiplications  $\mathbf{Y} \leftarrow \mathbf{S}_\star \mathbf{X}$ ,  $\mathbf{Y} \leftarrow \mathbf{M}_\star \mathbf{X}$  and approximating the action of inverses in the form  $\mathbf{y} \leftarrow (\sigma \mathbf{M}_\star - \mathbf{S}_\star)^{-1} \mathbf{x}$ ).

Taking this into account, instead of (5) we consider a perturbed<sup>1</sup> problem

$$\underbrace{\begin{bmatrix} \mathbf{A} & \mathbf{B}^T \\ \mathbf{B} & -\mathbf{C}_\star \end{bmatrix}}_{\mathcal{A}_\star :=} \begin{bmatrix} \mathbf{x} \\ \mathbf{y} \end{bmatrix} = \mu \underbrace{\begin{bmatrix} \epsilon \mathbf{A} & \\ & \mathbf{M}_\star \end{bmatrix}}_{\mathcal{M}_\star^\epsilon :=} \begin{bmatrix} \mathbf{x} \\ \mathbf{y} \end{bmatrix} \tag{6}$$

with  $0 < \epsilon \ll 1$ . For  $\mathcal{A}_0$  and  $\mathcal{M}_0^\epsilon$  we have

$$\mu = -\lambda + o(1) \quad \text{or} \quad \epsilon^{-1} + \lambda + o(1), \quad \epsilon \rightarrow 0. \tag{7}$$

This makes it easy to pick only “correct” eigenvalues. To ease the computation further we replace the  $(1, 1)$ -block of  $\mathcal{M}_\star^\epsilon$  with  $\epsilon \mathbf{I}$ .

To make sure that results are consistent we solve (6) for  $\epsilon = 10^{-5}$  and  $\epsilon = 10^{-6}$ ; for the coarse mesh levels we also check that the dense solver for (5) and the iterative one for (6) give solutions that coincide.

### 1.3 Numerical results: dependency of the spectrum on the mesh size

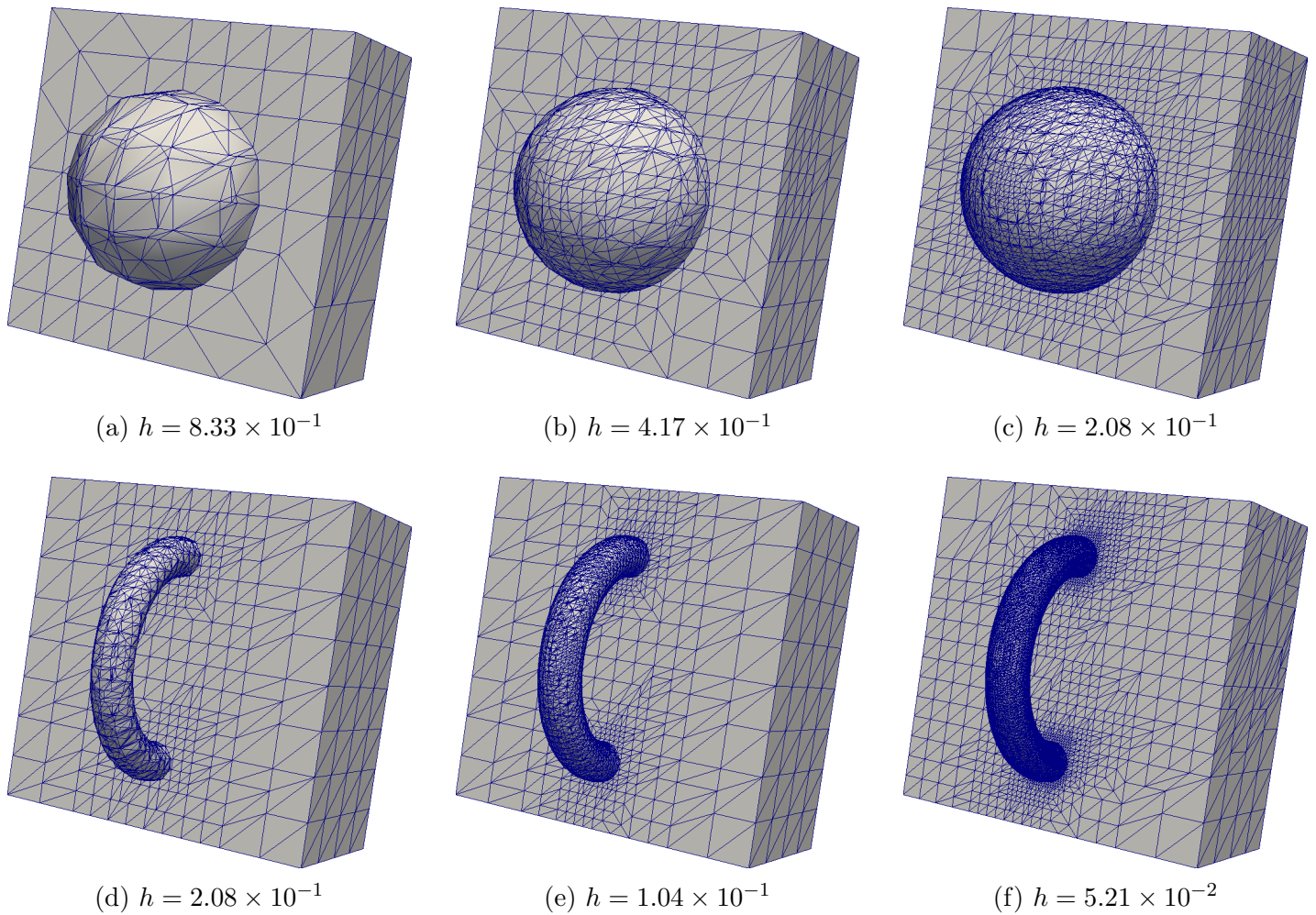


Figure 1: First three mesh levels for  $\Gamma_{\text{sph}}$  (top) and  $\Gamma_{\text{tor}}$  (bottom)

---

<sup>1</sup>The majority of generalized eigenvalue solvers require left-hand-side matrix to be Hermitian and right-hand-side matrix to be Hermitian **positive definite**; that’s why we need to introduce  $\epsilon > 0$ .

Table 1: Spectrum of (5) for  $\mathbf{P}_1 - P_1$ 

 (a)  $\Gamma = \Gamma_{\text{sph}}$ 

$h$	$n_{\mathbf{A}}$	$n_{\mathbf{S}}$	$\mathbf{S}_0$		$\mathbf{S}_n$		$\mathbf{S}_{\text{full}}$	
			$\lambda_2$	$\lambda_{n_{\mathbf{S}}}$	$\lambda_2$	$\lambda_{n_{\mathbf{S}}}$	$\lambda_2$	$\lambda_{n_{\mathbf{S}}}$
$8.33 \times 10^{-1}$	153	51	$1.32 \times 10^{-2}$	1.42	$7.48 \times 10^{-1}$	1.13	$9.58 \times 10^{-1}$	1.06
$4.17 \times 10^{-1}$	570	190	$5.12 \times 10^{-3}$	1.04	$5.77 \times 10^{-1}$	1.	$8.54 \times 10^{-1}$	1.
$2.08 \times 10^{-1}$	1992	664	$4.4 \times 10^{-3}$	$7.93 \times 10^{-1}$	$3.87 \times 10^{-1}$	1.	$6.71 \times 10^{-1}$	1.
$1.04 \times 10^{-1}$	8292	2764	$2.01 \times 10^{-3}$	$7.79 \times 10^{-1}$	$2.19 \times 10^{-1}$	1.	$5.82 \times 10^{-1}$	1.
$5.21 \times 10^{-2}$	32736	10912	$6.04 \times 10^{-5}$	$9.81 \times 10^{-1}$	$1.17 \times 10^{-1}$	1.	$5.37 \times 10^{-1}$	1.
$2.6 \times 10^{-2}$	131592	43864	$3.53 \times 10^{-5}$	$8.67 \times 10^{-1}$	$5.72 \times 10^{-2}$	1.	$5.16 \times 10^{-1}$	1.
$1.3 \times 10^{-2}$	525864	175288	$2.16 \times 10^{-6}$	$7.34 \times 10^{-1}$	$2.84 \times 10^{-2}$	1.	$5.04 \times 10^{-1}$	1.

 (b)  $\Gamma = \Gamma_{\text{tor}}$ 

$h$	$n_{\mathbf{A}}$	$n_{\mathbf{S}}$	$\mathbf{S}_0$		$\mathbf{S}_n$		$\mathbf{S}_{\text{full}}$	
			$\lambda_2$	$\lambda_{n_{\mathbf{S}}}$	$\lambda_2$	$\lambda_{n_{\mathbf{S}}}$	$\lambda_2$	$\lambda_{n_{\mathbf{S}}}$
$2.08 \times 10^{-1}$	972	324	$5.04 \times 10^{-2}$	4.93	$2.84 \times 10^{-1}$	1.35	$3.64 \times 10^{-1}$	1.19
$1.04 \times 10^{-1}$	4740	1580	$2.99 \times 10^{-3}$	3.83	$1.58 \times 10^{-1}$	1.02	$3.35 \times 10^{-1}$	1.01
$5.21 \times 10^{-2}$	19704	6568	$1.11 \times 10^{-3}$	5.45	$7.73 \times 10^{-2}$	1.01	$3.25 \times 10^{-1}$	1.
$2.6 \times 10^{-2}$	80808	26936	$1.2 \times 10^{-4}$	5.42	$3.07 \times 10^{-2}$	1.01	$3.21 \times 10^{-1}$	1.
$1.3 \times 10^{-2}$	327036	109012	$1.77 \times 10^{-5}$	5.23	$1.18 \times 10^{-2}$	1.01	$3.16 \times 10^{-1}$	1.

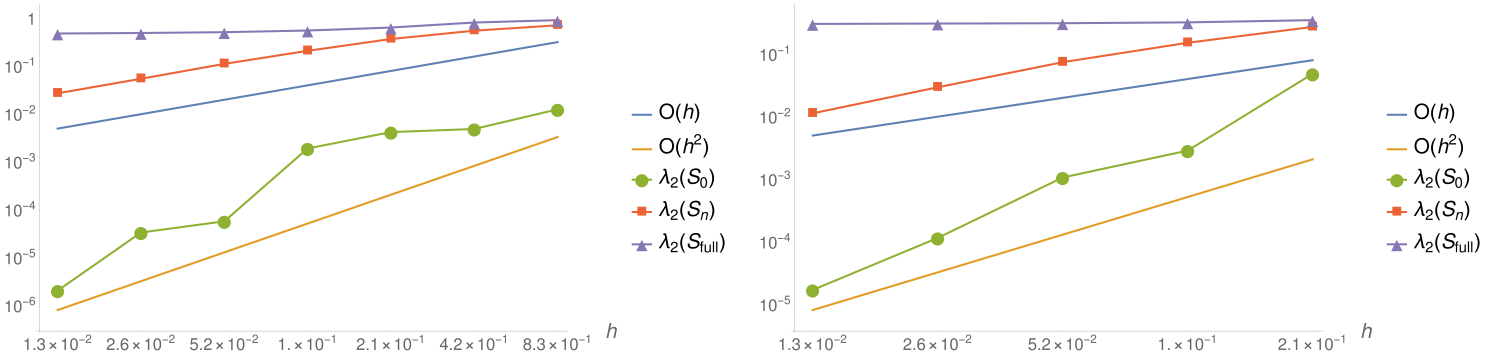

 Figure 2: Log-log plot of  $\lambda_2$  for Tables 1a (left) and 1b (right)

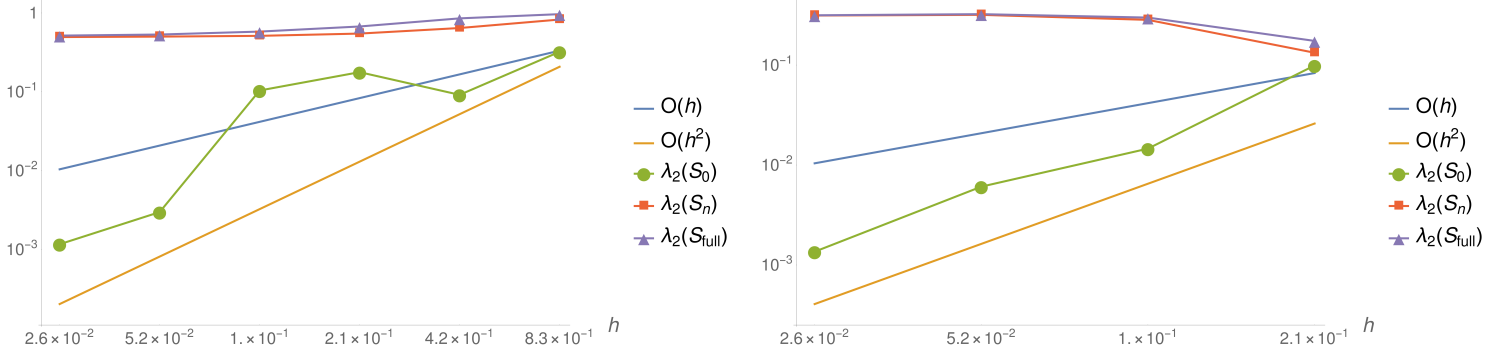
Table 2: Spectrum of (5) for  $\mathbf{P}_2 - P_1$ 

 (a)  $\Gamma = \Gamma_{\text{sph}}$ 

$h$	$n_{\mathbf{A}}$	$n_{\mathbf{S}}$	$\mathbf{S}_0$		$\mathbf{S}_n$		$\mathbf{S}_{\text{full}}$	
			$\lambda_2$	$\lambda_{n_{\mathbf{S}}}$	$\lambda_2$	$\lambda_{n_{\mathbf{S}}}$	$\lambda_2$	$\lambda_{n_{\mathbf{S}}}$
$8.33 \times 10^{-1}$	789	51	$3.22 \times 10^{-1}$	1.73	$8.27 \times 10^{-1}$	1.17	$9.68 \times 10^{-1}$	1.07
$4.17 \times 10^{-1}$	3240	190	$9.17 \times 10^{-2}$	1.08	$6.45 \times 10^{-1}$	1.	$8.56 \times 10^{-1}$	1.
$2.08 \times 10^{-1}$	11718	664	$1.78 \times 10^{-1}$	$8.31 \times 10^{-1}$	$5.49 \times 10^{-1}$	1.	$6.75 \times 10^{-1}$	1.
$1.04 \times 10^{-1}$	48762	2764	$1.04 \times 10^{-1}$	$8.35 \times 10^{-1}$	$5.14 \times 10^{-1}$	1.	$5.82 \times 10^{-1}$	1.
$5.21 \times 10^{-2}$	193014	10912	$2.99 \times 10^{-3}$	$9.89 \times 10^{-1}$	$5.02 \times 10^{-1}$	1.	$5.34 \times 10^{-1}$	1.
$2.6 \times 10^{-2}$	775998	43864	$1.17 \times 10^{-3}$	$7.9 \times 10^{-1}$	$4.96 \times 10^{-1}$	1.	$5.17 \times 10^{-1}$	1.

 (b)  $\Gamma = \Gamma_{\text{tor}}$ 

$h$	$n_{\mathbf{A}}$	$n_{\mathbf{S}}$	$\mathbf{S}_0$		$\mathbf{S}_n$		$\mathbf{S}_{\text{full}}$	
			$\lambda_2$	$\lambda_{n_{\mathbf{S}}}$	$\lambda_2$	$\lambda_{n_{\mathbf{S}}}$	$\lambda_2$	$\lambda_{n_{\mathbf{S}}}$
$2.08 \times 10^{-1}$	5184	324	$9.92 \times 10^{-2}$	3.89	$1.33 \times 10^{-1}$	1.37	$1.75 \times 10^{-1}$	1.19
$1.04 \times 10^{-1}$	27906	1580	$1.46 \times 10^{-2}$	4.35	$2.84 \times 10^{-1}$	1.04	$2.99 \times 10^{-1}$	1.02
$5.21 \times 10^{-2}$	116568	6568	$6.08 \times 10^{-3}$	4.85	$3.19 \times 10^{-1}$	1.01	$3.24 \times 10^{-1}$	1.01
$2.6 \times 10^{-2}$	477660	26936	$1.36 \times 10^{-3}$	4.92	$3.14 \times 10^{-1}$	1.01	$3.16 \times 10^{-1}$	1.


 Figure 3: Log-log plot of  $\lambda_2$  for Tables 2a (left) and 2b (right)

## 1.4 Numerical results: sensitivity of the spectrum to levelset shifts

In this section we investigate the sensitivity of the spectrum to levelset shifts

$$\Gamma \mapsto \Gamma + \alpha \mathbf{s}, \quad (8)$$

for some  $\alpha \in \mathbb{R}$  and  $\mathbf{s} \in \mathbb{R}^3$ ,  $\|\mathbf{s}\| = 1$ .

We construct the bulk mesh  $\Omega_h^\Gamma$  and then perform the assembly of matrices (1) using the shifted levelset (8). That is, the refinement of  $\Omega_h^\Gamma$  is performed using  $\Gamma$ , not  $\Gamma + \alpha \mathbf{s}$ , and  $\Omega_h^{\Gamma+\alpha \mathbf{s}}$  is never constructed. We choose  $\alpha \in [0, h]$  to guarantee the appearance of “small cuts” in  $\Omega_h^\Gamma$ .

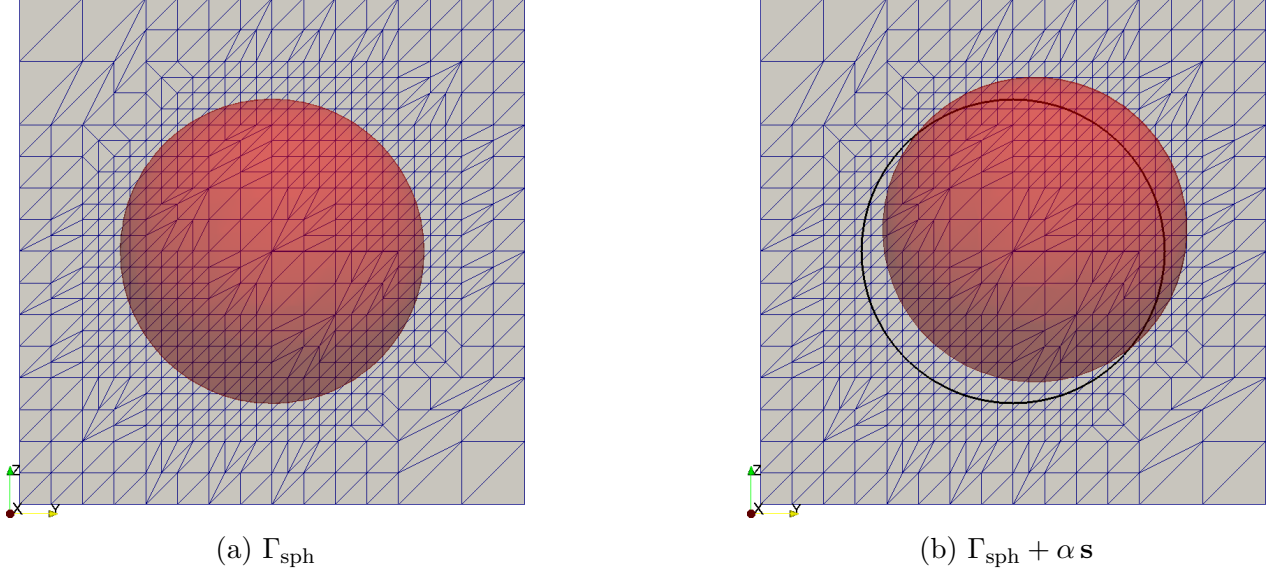


Figure 4: The unit sphere (left) and the shifted unit sphere (right). Here  $\mathbf{s} = (0, 1, 1)^T / \sqrt{2}$ ,  $\alpha = 0.2$ , and  $h = 2.08 \times 10^{-1}$ . The bulk mesh  $\Omega_h^\Gamma$  is computed for  $\Gamma_{\text{sph}}$  and then used for  $\Gamma_{\text{sph}} + \alpha \mathbf{s}$

Table 3: Spectrum of (5) for perturbed levelset  $\Gamma_{\text{sph}} + \alpha \mathbf{s}$ . Here  $\mathbf{s} = (1, 1, 1)^T / \sqrt{3}$ ,  $h = 1.04 \times 10^{-1}$

(a)  $\mathbf{P}_1 - P_1$

Surface	$\mathbf{S}_0$		$\mathbf{S}_n$		$\mathbf{S}_{\text{full}}$	
	$\lambda_2$	$\lambda_{n\mathbf{S}}$	$\lambda_2$	$\lambda_{n\mathbf{S}}$	$\lambda_2$	$\lambda_{n\mathbf{S}}$
$\Gamma_{\text{sph}}$	$2.006 \times 10^{-3}$	$7.79 \times 10^{-1}$	$2.19 \times 10^{-1}$	1.	$5.818 \times 10^{-1}$	1.
$\Gamma_{\text{sph}} + 0.1 h \mathbf{s}$	$4.832 \times 10^{-4}$	$8.01 \times 10^{-1}$	$2.195 \times 10^{-1}$	1.	$5.818 \times 10^{-1}$	1.
$\Gamma_{\text{sph}} + 0.3 h \mathbf{s}$	$7.278 \times 10^{-4}$	$8.17 \times 10^{-1}$	$2.203 \times 10^{-1}$	1.	$5.818 \times 10^{-1}$	1.
$\Gamma_{\text{sph}} + 0.5 h \mathbf{s}$	$3.121 \times 10^{-4}$	$8.67 \times 10^{-1}$	$2.221 \times 10^{-1}$	1.	$5.82 \times 10^{-1}$	1.
$\Gamma_{\text{sph}} + 0.7 h \mathbf{s}$	$1.438 \times 10^{-3}$	1.51	$2.254 \times 10^{-1}$	1.	$5.82 \times 10^{-1}$	1.
$\Gamma_{\text{sph}} + h \mathbf{s}$	$1.79 \times 10^{-3}$	2.07	$2.332 \times 10^{-1}$	1.	$5.827 \times 10^{-1}$	1.

(b)  $\mathbf{P}_2 - P_1$

Surface	$\mathbf{S}_0$		$\mathbf{S}_n$		$\mathbf{S}_{\text{full}}$	
	$\lambda_2$	$\lambda_{n\mathbf{S}}$	$\lambda_2$	$\lambda_{n\mathbf{S}}$	$\lambda_2$	$\lambda_{n\mathbf{S}}$
$\Gamma_{\text{sph}}$	$1.041 \times 10^{-1}$	$8.35 \times 10^{-1}$	$5.138 \times 10^{-1}$	1.	$5.841 \times 10^{-1}$	1.
$\Gamma_{\text{sph}} + 0.1 h \mathbf{s}$	$1.705 \times 10^{-3}$	$8.58 \times 10^{-1}$	$5.138 \times 10^{-1}$	1.	$5.841 \times 10^{-1}$	1.
$\Gamma_{\text{sph}} + 0.3 h \mathbf{s}$	$2.293 \times 10^{-3}$	$8.81 \times 10^{-1}$	$5.137 \times 10^{-1}$	1.	$5.841 \times 10^{-1}$	1.
$\Gamma_{\text{sph}} + 0.5 h \mathbf{s}$	$5.63 \times 10^{-3}$	$9.35 \times 10^{-1}$	$5.138 \times 10^{-1}$	1.	$5.844 \times 10^{-1}$	1.
$\Gamma_{\text{sph}} + 0.7 h \mathbf{s}$	$8.188 \times 10^{-3}$	1.77	$5.138 \times 10^{-1}$	1.	$5.843 \times 10^{-1}$	1.
$\Gamma_{\text{sph}} + h \mathbf{s}$	$1.93 \times 10^{-2}$	2.21	$5.142 \times 10^{-1}$	1.	$5.852 \times 10^{-1}$	1.

## 2 Convergence results

We solve model problem from [1, p. 20]. We set

$$\begin{aligned}\tilde{\mathbf{u}}(x, y, z) &:= (-z^2, y, x)^T, \\ \tilde{p}(x, y, z) &:= x y^2 + z, \\ \phi(\mathbf{x}) &:= \|\mathbf{x}\|^2 - 1.\end{aligned}\tag{9}$$

The exact solution on the unit sphere is chosen as

$$\mathbf{u}(\mathbf{x}) := \mathbf{P} \tilde{\mathbf{u}}\left(\frac{\mathbf{x}}{\|\mathbf{x}\|}\right), \quad p(\mathbf{x}) := \tilde{p}\left(\frac{\mathbf{x}}{\|\mathbf{x}\|}\right).\tag{10}$$

This way we “extend” (9) radially. It is useful since we use *the approximation* of  $\Gamma_{\text{sph}}$ .

### 2.1 $\mathbf{P}_1 - P_1$ Trace FEM

Here we compare approaches (16) and (17). We use one virtual refinement for surface integrals,  $m = 2$ , so we have  $\Gamma_{h/2}^{2 \rightarrow 1} = \Gamma_{h/2}^1$  (see (13) and (15)). We use the full stabilization matrix  $\mathbf{C}_{\text{full}}$ . Note that  $\phi \in P_2$  in (9), and hence  $\Gamma_h^2 = \Gamma$ . Thus (16) boils down to

$$\begin{aligned}\langle \mathbf{A} \vec{\mathbf{u}}, \vec{\mathbf{v}} \rangle &= \int_{\Gamma_{h/2}^1}^5 (E_{s, \Gamma}(\mathbf{u}) : E_{s, \Gamma}(\mathbf{v}) + \mathbf{u} \cdot \mathbf{v} + \tau (\mathbf{u} \cdot \mathbf{n}_\Gamma) (\mathbf{v} \cdot \mathbf{n}_\Gamma)) \, ds \\ &\quad + \rho_u \int_{\Omega_h^\Gamma}^5 \frac{\partial \mathbf{u}}{\partial \mathbf{n}_\Gamma} \cdot \frac{\partial \mathbf{v}}{\partial \mathbf{n}_\Gamma} \, d\mathbf{x}, \quad \mathbf{A} \in \mathbb{R}^{n_{\mathbf{A}} \times n_{\mathbf{A}}}, \\ \langle \mathbf{B} \vec{\mathbf{u}}, \vec{\mathbf{q}} \rangle &= - \int_{\Gamma_{h/2}^1}^5 q \, \text{div}_\Gamma \mathbf{u} \, ds, \quad \mathbf{B} \in \mathbb{R}^{n_{\mathbf{S}} \times n_{\mathbf{A}}}, \\ \langle \mathbf{M}_0 \vec{\mathbf{p}}, \vec{\mathbf{q}} \rangle &= \int_{\Gamma_{h/2}^1}^5 p \, q \, ds, \quad \mathbf{M}_0 \in \mathbb{R}^{n_{\mathbf{S}} \times n_{\mathbf{S}}}, \\ \langle \mathbf{C}_{\text{full}} \vec{\mathbf{p}}, \vec{\mathbf{q}} \rangle &= \rho_p \int_{\Omega_h^\Gamma}^5 \nabla p \cdot \nabla q \, d\mathbf{x}, \quad \mathbf{C}_{\text{full}} \in \mathbb{R}^{n_{\mathbf{S}} \times n_{\mathbf{S}}},\end{aligned}\tag{11}$$

and e.g. the integrand that involves  $E_{s, \Gamma} \equiv E_s$  is exact. Similarly, approach (17) boils down to

$$\begin{aligned}\langle \mathbf{A} \vec{\mathbf{u}}, \vec{\mathbf{v}} \rangle &= \int_{\Gamma_{h/2}^1}^5 (E_{s, \Gamma_{h/2}^1}(\mathbf{u}) : E_{s, \Gamma_{h/2}^1}(\mathbf{v}) + \mathbf{u} \cdot \mathbf{v} + \tau (\mathbf{u} \cdot \mathbf{n}_\Gamma) (\mathbf{v} \cdot \mathbf{n}_\Gamma)) \, ds \\ &\quad + \rho_u \int_{\Omega_h^\Gamma}^5 \frac{\partial \mathbf{u}}{\partial \mathbf{n}_\Gamma} \cdot \frac{\partial \mathbf{v}}{\partial \mathbf{n}_\Gamma} \, d\mathbf{x}, \quad \mathbf{A} \in \mathbb{R}^{n_{\mathbf{A}} \times n_{\mathbf{A}}}, \\ \langle \mathbf{B} \vec{\mathbf{u}}, \vec{\mathbf{q}} \rangle &= - \int_{\Gamma_{h/2}^1}^5 q \, \text{div}_{\Gamma_{h/2}^1} \mathbf{u} \, ds, \quad \mathbf{B} \in \mathbb{R}^{n_{\mathbf{S}} \times n_{\mathbf{A}}}, \\ \langle \mathbf{M}_0 \vec{\mathbf{p}}, \vec{\mathbf{q}} \rangle &= \int_{\Gamma_{h/2}^1}^5 p \, q \, ds, \quad \mathbf{M}_0 \in \mathbb{R}^{n_{\mathbf{S}} \times n_{\mathbf{S}}}, \\ \langle \mathbf{C}_{\text{full}} \vec{\mathbf{p}}, \vec{\mathbf{q}} \rangle &= \rho_p \int_{\Omega_h^\Gamma}^5 \nabla p \cdot \nabla q \, d\mathbf{x}, \quad \mathbf{C}_{\text{full}} \in \mathbb{R}^{n_{\mathbf{S}} \times n_{\mathbf{S}}}.\end{aligned}\tag{12}$$



Table 4: Convergence results. Matrices are assembled as in (11) (top table) and (12) (bottom table)

$m$	$h$	$\ \mathbf{u} - \mathbf{u}_h\ _{\mathbb{H}^1(\Gamma)}$	Order	$\ \mathbf{u} - \mathbf{u}_h\ _{\mathbb{L}^2(\Gamma)}$	Order	$\ p - p_h\ _{\mathbb{L}^2(\Gamma)}$	Order
2	$8.33 \times 10^{-1}$	3.4		2.2		1.1	
	$4.17 \times 10^{-1}$	1.8	$9.39 \times 10^{-1}$	1.1	$9.57 \times 10^{-1}$	$9.3 \times 10^{-1}$	$2.56 \times 10^{-1}$
	$2.08 \times 10^{-1}$	$7.6 \times 10^{-1}$	1.23	$3.6 \times 10^{-1}$	1.65	$5.1 \times 10^{-1}$	$8.75 \times 10^{-1}$
	$1.04 \times 10^{-1}$	$3.1 \times 10^{-1}$	1.3	$1. \times 10^{-1}$	1.85	$1.8 \times 10^{-1}$	1.46
	$5.21 \times 10^{-2}$	$1.3 \times 10^{-1}$	1.21	$2.6 \times 10^{-2}$	1.95	$5.3 \times 10^{-2}$	1.79
	$2.6 \times 10^{-2}$	$6.4 \times 10^{-2}$	1.05	$6.5 \times 10^{-3}$	1.98	$1.5 \times 10^{-2}$	1.84
	$1.3 \times 10^{-2}$	$3.2 \times 10^{-2}$	1.01	$1.7 \times 10^{-3}$	1.97	$6.6 \times 10^{-3}$	1.17
	$6.51 \times 10^{-3}$	$1.6 \times 10^{-2}$	$9.93 \times 10^{-1}$	$5.1 \times 10^{-4}$	1.72	$5.5 \times 10^{-3}$	$2.59 \times 10^{-1}$
4	$6.51 \times 10^{-3}$	$1.7 \times 10^{-2}$	$9.2 \times 10^{-1}$	$4.1 \times 10^{-4}$	2.02	$1.6 \times 10^{-3}$	2.06

$h$	$\ \mathbf{u} - \mathbf{u}_h\ _{\mathbb{H}^1(\Gamma)}$	Order	$\ \mathbf{u} - \mathbf{u}_h\ _{\mathbb{L}^2(\Gamma)}$	Order	$\ p - p_h\ _{\mathbb{L}^2(\Gamma)}$	Order
$8.33 \times 10^{-1}$	3.4		2.2		1.1	
$4.17 \times 10^{-1}$	1.8	$9.28 \times 10^{-1}$	1.1	$9.3 \times 10^{-1}$	$9.3 \times 10^{-1}$	$2.58 \times 10^{-1}$
$2.08 \times 10^{-1}$	$7.6 \times 10^{-1}$	1.23	$3.6 \times 10^{-1}$	1.65	$5.1 \times 10^{-1}$	$8.62 \times 10^{-1}$
$1.04 \times 10^{-1}$	$3.1 \times 10^{-1}$	1.29	$1. \times 10^{-1}$	1.85	$1.9 \times 10^{-1}$	1.44
$5.21 \times 10^{-2}$	$1.3 \times 10^{-1}$	1.22	$2.6 \times 10^{-2}$	1.94	$5.5 \times 10^{-2}$	1.77
$2.6 \times 10^{-2}$	$6.4 \times 10^{-2}$	1.07	$6.7 \times 10^{-3}$	1.97	$1.5 \times 10^{-2}$	1.89
$1.3 \times 10^{-2}$	$3.1 \times 10^{-2}$	1.02	$1.7 \times 10^{-3}$	1.98	$4. \times 10^{-3}$	1.89
$6.51 \times 10^{-3}$	$1.5 \times 10^{-2}$	1.02	$4.3 \times 10^{-4}$	1.99	$1.2 \times 10^{-3}$	1.77

Table 5: Solver statistics for (11) (left table) and (12) (right table)

$h$	Outer iterations	Residual norm
$8.33 \times 10^{-1}$	14	$1. \times 10^{-8}$
$4.17 \times 10^{-1}$	20	$9.2 \times 10^{-9}$
$2.08 \times 10^{-1}$	26	$8.8 \times 10^{-9}$
$1.04 \times 10^{-1}$	29	$5.4 \times 10^{-9}$
$5.21 \times 10^{-2}$	29	$7.1 \times 10^{-9}$
$2.6 \times 10^{-2}$	29	$4.5 \times 10^{-9}$
$1.3 \times 10^{-2}$	27	$9.5 \times 10^{-9}$
$6.51 \times 10^{-3}$	30	$6.5 \times 10^{-9}$

$h$	Outer iterations	Residual norm
$8.33 \times 10^{-1}$	15	$1.7 \times 10^{-9}$
$4.17 \times 10^{-1}$	20	$7.7 \times 10^{-9}$
$2.08 \times 10^{-1}$	26	$7. \times 10^{-9}$
$1.04 \times 10^{-1}$	29	$4.3 \times 10^{-9}$
$5.21 \times 10^{-2}$	29	$5.2 \times 10^{-9}$
$2.6 \times 10^{-2}$	27	$8.5 \times 10^{-9}$
$1.3 \times 10^{-2}$	27	$3.6 \times 10^{-9}$
$6.51 \times 10^{-3}$	29	$7.4 \times 10^{-9}$

For statistics: using 64 CPUs, computation of the meshlevel 6 ( $h = 2.6 \times 10^{-2}$ ) takes  $\sim 14$  minutes, meshlevel 7 takes  $\sim 75$  minutes, and meshlevel 8 takes  $\sim 7.3$  hours.

The errors in Table 4 are computed as explained in section 3.6.

## 2.2 $P_2 - P_1$ Trace FEM

We use the normal stabilization matrix  $\mathbf{C}_n$ . We stick to approach (17). We choose  $m = O(h^{-1/2})$  so that the geometric error is  $O(h^3)$ . Thus  $m = 2, 2, 4, 4, 6, 8, 10, 14$  for meshlevel 1, 2 and so forth, respectively.

Table 6: Convergence results.  $\tau = h^{-2}$ ,  $\rho_u = \rho_p = h$

$h$	$\ \mathbf{u} - \mathbf{u}_h\ _{\mathbb{H}^1(\Gamma)}$	Order	$\ \mathbf{u} - \mathbf{u}_h\ _{\mathbb{L}^2(\Gamma)}$	Order	$\ p - p_h\ _{\mathbb{L}^2(\Gamma)}$	Order
$8.33 \times 10^{-1}$	2.8		1.7		2.1	
$4.17 \times 10^{-1}$	1.9	$5.74 \times 10^{-1}$	$9. \times 10^{-1}$	$9.15 \times 10^{-1}$	1.7	$2.57 \times 10^{-1}$
$2.08 \times 10^{-1}$	$7.2 \times 10^{-1}$	1.37	$3.4 \times 10^{-1}$	1.39	$7.1 \times 10^{-1}$	1.31
$1.04 \times 10^{-1}$	$2.2 \times 10^{-1}$	1.7	$1. \times 10^{-1}$	1.78	$2.1 \times 10^{-1}$	1.76
$5.21 \times 10^{-2}$	$6.2 \times 10^{-2}$	1.85	$2.6 \times 10^{-2}$	1.92	$5.1 \times 10^{-2}$	2.04
$2.6 \times 10^{-2}$	$1.8 \times 10^{-2}$	1.81	$6.5 \times 10^{-3}$	2.01	$1.3 \times 10^{-2}$	1.91

$h$	$\ \mathbf{u}_h \cdot \mathbf{n}\ _{\mathbb{L}^2(\Gamma)}$	Order	Outer iterations	Residual norm
$8.33 \times 10^{-1}$	1.7		24	$9.9 \times 10^{-9}$
$4.17 \times 10^{-1}$	$8.9 \times 10^{-1}$	$8.87 \times 10^{-1}$	31	$4.6 \times 10^{-9}$
$2.08 \times 10^{-1}$	$3.4 \times 10^{-1}$	1.38	31	$4.5 \times 10^{-9}$
$1.04 \times 10^{-1}$	$1. \times 10^{-1}$	1.78	29	$3.5 \times 10^{-9}$
$5.21 \times 10^{-2}$	$2.6 \times 10^{-2}$	1.95	27	$6.9 \times 10^{-9}$
$2.6 \times 10^{-2}$	$6.5 \times 10^{-3}$	1.99	28	$7.3 \times 10^{-9}$

Table 7: Convergence results.  $\tau = h^{-3}$ ,  $\rho_u = \rho_p = h$

$h$	$\ \mathbf{u} - \mathbf{u}_h\ _{\mathbb{H}^1(\Gamma)}$	Order	$\ \mathbf{u} - \mathbf{u}_h\ _{\mathbb{L}^2(\Gamma)}$	Order	$\ p - p_h\ _{\mathbb{L}^2(\Gamma)}$	Order
$8.33 \times 10^{-1}$	2.7		1.6		2.	
$4.17 \times 10^{-1}$	1.2	1.2	$5.3 \times 10^{-1}$	1.61	1.	$9.82 \times 10^{-1}$
$2.08 \times 10^{-1}$	$2.4 \times 10^{-1}$	2.26	$8.5 \times 10^{-2}$	2.66	$1.9 \times 10^{-1}$	2.44
$1.04 \times 10^{-1}$	$7.5 \times 10^{-2}$	1.68	$1.2 \times 10^{-2}$	2.87	$2.8 \times 10^{-2}$	2.74
$5.21 \times 10^{-2}$	$3. \times 10^{-2}$	1.32	$5.1 \times 10^{-3}$	1.19	$4.6 \times 10^{-3}$	2.62
$2.6 \times 10^{-2}$	$1.1 \times 10^{-2}$	1.43	$3. \times 10^{-4}$	4.09	$1.4 \times 10^{-3}$	1.69
$1.3 \times 10^{-2}$	$4.7 \times 10^{-3}$	1.24	$6.6 \times 10^{-5}$	2.18	$6.2 \times 10^{-4}$	1.18

$h$	$\ \mathbf{u}_h \cdot \mathbf{n}\ _{\mathbb{L}^2(\Gamma)}$	Order	Outer iterations	Residual norm
$8.33 \times 10^{-1}$	1.6		25	$4.4 \times 10^{-9}$
$4.17 \times 10^{-1}$	$5.2 \times 10^{-1}$	1.61	32	$3.6 \times 10^{-9}$
$2.08 \times 10^{-1}$	$8.4 \times 10^{-2}$	2.63	31	$5.9 \times 10^{-9}$
$1.04 \times 10^{-1}$	$1.1 \times 10^{-2}$	2.91	28	$9.6 \times 10^{-9}$
$5.21 \times 10^{-2}$	$1.4 \times 10^{-3}$	3.01	27	$7.4 \times 10^{-9}$
$2.6 \times 10^{-2}$	$1.7 \times 10^{-4}$	3.01	27	$3.3 \times 10^{-9}$
$1.3 \times 10^{-2}$	$2.1 \times 10^{-5}$	3.	33	$8.8 \times 10^{-9}$

Table 8: Convergence results.  $\tau = 0.1 h^{-3}$ ,  $\rho_u = \rho_p = h$ 

$h$	$\ \mathbf{u} - \mathbf{u}_h\ _{\mathbb{H}^1(\Gamma)}$	Order	$\ \mathbf{u} - \mathbf{u}_h\ _{\mathbb{L}^2(\Gamma)}$	Order	$\ p - p_h\ _{\mathbb{L}^2(\Gamma)}$	Order
$8.33 \times 10^{-1}$	3.4		2.1		2.6	
$4.17 \times 10^{-1}$	3.	$1.96 \times 10^{-1}$	1.5	$5.02 \times 10^{-1}$	2.9	$-1.44 \times 10^{-1}$
$2.08 \times 10^{-1}$	1.2	1.29	$6. \times 10^{-1}$	1.32	1.2	1.25
$1.04 \times 10^{-1}$	$2.3 \times 10^{-1}$	2.42	$1. \times 10^{-1}$	2.53	$2.2 \times 10^{-1}$	2.5

$h$	$\ \mathbf{u}_h \cdot \mathbf{n}\ _{\mathbb{L}^2(\Gamma)}$	Order	Outer iterations	Residual norm
$8.33 \times 10^{-1}$	2.1		25	$5.8 \times 10^{-9}$
$4.17 \times 10^{-1}$	1.5	$4.69 \times 10^{-1}$	30	$4.8 \times 10^{-9}$
$2.08 \times 10^{-1}$	$6. \times 10^{-1}$	1.32	30	$5.6 \times 10^{-9}$
$1.04 \times 10^{-1}$	$1. \times 10^{-1}$	2.53	29	$3.5 \times 10^{-9}$

For statistics: using 64 CPUs, computation of the meshlevel 3 ( $h = 2.08 \times 10^{-1}$ ) takes  $\sim 1$  minute, meshlevel 4 takes  $\sim 7$  minutes, meshlevel 5 takes  $\sim 50$  minutes, meshlevel 6 takes 4.8 hours, and meshlevel 7 takes  $\sim 21.3$  hours.

### 3 Notes on DROPS implementation

#### 3.1 Notations

We denote by  $P_h^n \subset \bar{P}_h^n$  spaces of continuous and discontinuous nodal  $P_n$  interpolants defined on  $\Omega_\Gamma^h$ , respectively. For a function  $f$ ,  $I_h^n(f) \in P_h^n$  is the corresponding interpolant; we will use the notation  $f_h^n$  to emphasize that  $f_h^n \in P_h^n$  and  $f_h^n$  approximates  $f$  in some sense, but  $I_h^n(f) \neq f_h^n$ .

We set

$$\Gamma_h^n := \{\mathbf{x} \in \mathbb{R}^3 : (I_h^n(\phi))(\mathbf{x}) = 0\}, \quad (13)$$

$$\mathbf{n}_{\Gamma_h^n} = \frac{\nabla I_h^n(\phi)}{\|\nabla I_h^n(\phi)\|} \notin \bar{P}_h^m \text{ for any } m \text{ if } n > 1. \quad (14)$$

Note that  $\Gamma_h^n$  is a continuous piecewise  $P_n$  surface in  $\Omega_\Gamma^h$ , and  $\Gamma_h^n \neq I_h^n(\Gamma)$ . The unit normal  $\mathbf{n}_{\Gamma_h^n}$  is not a rational function; it is continuous in  $T \in \Omega_\Gamma^h$  and discontinuous on faces. We also define

$$\Gamma_{h/m}^{2 \rightarrow 1} := \{\mathbf{x} \in \mathbb{R}^3 : (I_{h/m}^1(I_h^2(\phi)))(\mathbf{x}) = 0\}. \quad (15)$$

Note that  $I_{h/2}^1(I_h^2(\phi)) = I_{h/2}^1(\phi)$  (since in order to build both  $I_{h/2}^1$  and  $I_h^2$  the same values of  $\phi$  are used), and  $I_{h/m}^1(I_h^2(\phi)) \neq I_{h/m}^1(\phi)$  for  $m > 2$ . Thus we have  $\Gamma_{h/2}^{2 \rightarrow 1} = \Gamma_{h/2}^1$ , and  $\Gamma_{h/m}^{2 \rightarrow 1} \neq \Gamma_{h/m}^1$  for  $m > 2$ .

#### 3.2 Approximation of integrands involving $\mathbf{n}_\Gamma$

We start with description of the continuous levelset  $\phi$  of  $\Gamma = \{\mathbf{x} \in \mathbb{R}^3 : \phi(\mathbf{x}) = 0\}$ . It is stored in `levelset_fun` variable. For example, for the unit sphere we have:

```

// surfnavierstokes_funcs.h
DROPS::Point3DCL sphere_2_shift(0.);
double sphere_2 (const DROPS::Point3DCL& p, double) {
    return pow(p[0] - sphere_2_shift[0], 2.) +
           pow(p[1] - sphere_2_shift[1], 2.) +
           pow(p[2] - sphere_2_shift[2], 2.) - 1.;
}

// surfnavierstokes.cpp
instat_scalar_fun_ptr levelset_fun;
// ...
levelset_fun = &sphere_2;

```

Continuous piecewise  $P_2$  interpolant  $I_h^2(\phi)$  of  $\phi$  is built on  $\Omega_\Gamma^h$  via iterating over vertices and edges of  $\Omega_\Gamma^h$ . It is stored in `lset` object:

```

// levelset.cpp
void LevelsetP2ContCL::Init( instat_scalar_fun_ptr phi0, double t) {
    const Uint lvl= Phi.GetLevel(),
    idx= Phi.RowIdx->GetIdx();
    for (auto it = MG_.GetTriangVertexBegin(lvl), end = MG_.GetTriangVertexEnd(lvl); it
        != end; ++it) {
        if (it->Unknowns.Exist(idx))
            Phi.Data[it->Unknowns(idx)]= phi0( it->GetCoord(), t);
    }
    for (auto it = MG_.GetTriangEdgeBegin(lvl), end = MG_.GetTriangEdgeEnd(lvl); it !=
        end; ++it) {
        if (it->Unknowns.Exist(idx))
            Phi.Data[it->Unknowns(idx)]= phi0( GetBaryCenter( *it), t);
    }
}

// surfnavierstokes.cpp
DROPS::LevelsetP2CL& lset(*DROPS::LevelsetP2CL::Create(mg, lsbdn, sf));
// ...
lset.Init(levelset_fun);

```

In order to assemble matrices in (1) for e.g.  $\mathbf{P}_1 - P_1$  elements, one calls

```

| SetupNavierStokesIF_P1P1(mg, &A, /* ... */ lset.Phi, /* ... */);

```

(Interestingly enough, this function does not get `lset` object that represents the interpolant; it gets only `lset.Phi`, which is the object of type `VecDescCL`. `lset.Phi` is essentially just a vector of values of  $\phi$  at interpolation points (i.e. vertices and edges' centroids of  $\Omega_\Gamma^h$ ). That is, the assembling function above has no idea what `lset.Phi` actually represents: one may interpret it as an element of  $P_h^2$  or e.g.  $P_{h/2}^1$ . Who knows?..)

No interpolation is built explicitly for  $\mathbf{n}_{\Gamma_h^2}$  in (14); it is implicitly represented via `qnormal` data field:

```

// ifacetransp.cpp
class LocalStokesCL {
    // ...
    GridFunctionCL<Point3DCL> qnormal;
    // ...
}

```

`qnormal` object is essentially a set of values of type `Point3DCL` which are obtained by mapping a (vector valued) function to suitable quadrature nodes. This is how it is constructed:

```

// ifacetransp.cpp
void LocalStokesCL::Get_Normals(const LocalP2CL<>& ls, LocalP1CL<Point3DCL>& Normals) {

```

```

    for(int i=0; i<10 ; ++i)
        Normals+=ls[i]*P2Grad[i];
}
// ...
void LocalStokesCL::calcIntegrands(const SMatrixCL<3,3>& T, const LocalP2CL<>& ls,
    const TetraCL& tet) {
    // ...
    LocalP1CL<Point3DCL> Normals;
    Get_Normals(ls, Normals);
    resize_and_evaluate_on_vertexes (Normals, q2Ddomain, qnormal);
    for(Uint i=0; i<qnormal.size(); ++i)
        qnormal[i]= qnormal[i]/qnormal[i].norm();
    // ...
}

```

First  $\nabla I_h^2(\phi|_T)$  is built (locally for a tetrahedron  $T \in \Omega_T^h$  represented by `tet`) and saved to `Normals` object. `ls[i]` gives the value of  $\phi|_T$  at  $i$ th node (vertices and edges' centroids—there are 10 of them for tetrahedra), and `P2Grad[i]` represents the gradient of quadratic basis function which itself is linear. (Actually, it is sufficient to have  $4 < 10$  linear functions to represent  $\nabla I_h^2(\phi|_T)$ , but this is how it is implemented here.) Finally, `qnormal` object is built via evaluating `Normals` at quadrature nodes and normalization.

Objects `qnormal` for surface integrals and `q3Dnormal` for volume integrals are used in approximation of  $\mathbf{P} = \mathbf{I} - \mathbf{n}\mathbf{n}^T$ , normal derivatives, and taking-normal-components in (1). `q3Dnormal` is constructed as `qnormal` but for quadrature points of tetrahedrons, not triangles.

For one,  $\mathbf{P} \nabla f_h^2$ ,  $f_h^2 := P_2$  basis function on  $\Omega_T^h$ , is approximated via `qsurfP2grad` object:

```

// ifacetransp.cpp
void LocalStokesCL::calcIntegrands(/* ... */) {
    // ...
    for(int j=0; j<10 ;++j) {
        resize_and_evaluate_on_vertexes(P2Grad[j], q2Ddomain, qsurfP2grad[j]);
        qsurfP2grad[j]-= dot(qsurfP2grad[j], qnormal)*qnormal;
    }
    // ...
}

```

The term  $\int_{\Omega_T^h} \frac{\partial p}{\partial \mathbf{n}} \frac{\partial q}{\partial \mathbf{n}} d\mathbf{x}$  in (1) is computed as

```

// ifacetransp.cpp
void LocalStokesCL::setupA_P1_stab(double A_P1_stab[4][4], double absdet) {
    for (int i=0; i<4; ++i)
        for (int j=0; j<4; ++j)
            A_P1_stab[i][j] = quad(dot(q3Dnormal, q3DP1Grad[i])*dot(q3Dnormal, q3DP1Grad[j]),
                absdet, q3Ddomain, AllTetraC);
}

```

### 3.3 Quadrature rules for $\int_\Gamma$ and $\int_{\Omega_T^h}$

All the 3D integrals in (1) are computed via iteration over  $T \in \Omega_T^h$  without any virtual refinements. `q3Ddomain` object represents the set of quadrature nodes and weights:

```

// ifacetransp.cpp
void LocalStokesCL::calc3DIntegrands(/* ... */) {
    make_SimpleQuadDomain<Quad5DataCL> (q3Ddomain, AllTetraC);
    // ...
}

```

It is used e.g. in `setupA.P1_stab` above. 15 nodes and weights are used, and the quadrature is exact for functions in  $\bar{P}_h^5$ .

All the surface integrals are also computed via iteration over  $T \in \Omega_\Gamma^h$ , but using  $\Gamma_{h/2}^1$ . One extra “virtual” refinement is achieved via setting

```
// ifacetransp.cpp
LocalStokesCL(bool fullGradient)
: lat(PrincipalLatticeCL::instance(2))
, /* ... */ { /* ... */ }
```

`PrincipalLatticeCL::instance(2)` means that each edge of the tetrahedron  $T \in \Omega_\Gamma^h$  is split into 2 edges, and  $T$  is split into 8 smaller tetrahedrons. Changing 2 to 4 will give us  $\Gamma_{h/4}^{2 \rightarrow 1}$  from (15) and so forth. `q2Ddomain` object represents the set of quadrature nodes and weights:

```
// ifacetransp.cpp
void LocalStokesCL::calcIntegrands(/* ... */) {
    // ...
    evaluate_on_vertexes( ls, lat, Addr( ls_loc));
    spatch.make_patch<MergeCutPolicyCL>( lat, ls_loc);
    make_CompositeQuad5Domain2D ( q2Ddomain, spatch, tet);
    // ...
}
```

Each linear subsurface in  $T \in \Omega_\Gamma^h$  has 7 quadrature nodes and weights, and the quadrature rule is again exact for functions in  $\bar{P}_h^5$ .

`spatch` represents a set of triangles that form  $\Gamma_{h/2}^1$  inside  $T$ . That is, in order to approximate zeros of  $\phi$ ,  $I_{h/2}^1(I_h^2(\phi)) = I_{h/2}^1(\phi)$  is used:

```
// subtriangulation.h
// ...
const double edge_bary1_cut= ls0/(ls0 - ls1); // the root of the level set function on
the edge
// ...
```

Here  $l(x) := \text{ls0}(1 - x) + \text{ls1}x$  is a linear function defined on the master edge  $[0, 1]$ . Indeed, its root is  $x = \text{ls0}/(\text{ls0} - \text{ls1})$ .

### 3.4 Summary on the matrix assembly

The matrices in (1) are assembled as

$$\begin{aligned}
\langle \mathbf{A} \vec{\mathbf{u}}, \vec{\mathbf{v}} \rangle &= \int_{\Gamma_{h/m}^{2 \rightarrow 1}}^5 (E_{s, \Gamma_h^2}(\mathbf{u}) : E_{s, \Gamma_h^2}(\mathbf{v}) + \mathbf{u} \cdot \mathbf{v} + \tau(\mathbf{u} \cdot \mathbf{n}_{\Gamma_h^2})(\mathbf{v} \cdot \mathbf{n}_{\Gamma_h^2})) \, ds \\
&\quad + \rho_u \int_{\Omega_h^\Gamma}^5 \frac{\partial \mathbf{u}}{\partial \mathbf{n}_{\Gamma_h^2}} \cdot \frac{\partial \mathbf{v}}{\partial \mathbf{n}_{\Gamma_h^2}} \, d\mathbf{x}, \quad \mathbf{A} \in \mathbb{R}^{n_A \times n_A}, \\
\langle \mathbf{B} \vec{\mathbf{u}}, \vec{\mathbf{q}} \rangle &= - \int_{\Gamma_{h/m}^{2 \rightarrow 1}}^5 q \operatorname{div}_{\Gamma_h^2} \mathbf{u} \, ds, \quad \mathbf{B} \in \mathbb{R}^{n_S \times n_A}, \\
\langle \mathbf{M}_0 \vec{\mathbf{p}}, \vec{\mathbf{q}} \rangle &= \int_{\Gamma_{h/m}^{2 \rightarrow 1}}^5 p q \, ds, \quad \mathbf{M}_0 \in \mathbb{R}^{n_S \times n_S}, \\
\langle \mathbf{C}_n \vec{\mathbf{p}}, \vec{\mathbf{q}} \rangle &= \rho_p \int_{\Omega_h^\Gamma}^5 \frac{\partial p}{\partial \mathbf{n}_{\Gamma_h^2}} \frac{\partial q}{\partial \mathbf{n}_{\Gamma_h^2}} \, d\mathbf{x}, \quad \mathbf{C}_n \in \mathbb{R}^{n_S \times n_S}, \\
\langle \mathbf{C}_{\text{full}} \vec{\mathbf{p}}, \vec{\mathbf{q}} \rangle &= \rho_p \int_{\Omega_h^\Gamma}^5 \nabla p \cdot \nabla q \, d\mathbf{x}, \quad \mathbf{C}_{\text{full}} \in \mathbb{R}^{n_S \times n_S},
\end{aligned} \tag{16}$$

Comments:

- $\int_{\Gamma_{h/m}^{2 \rightarrow 1}}^5 \cdot \, ds$  denotes a composite quadrature rule that is exact for  $\bar{P}_h^5(\Gamma_{h/m}^{2 \rightarrow 1})$ , i.e. this quadrature is exact for piecewise polynomials up to degree 5 on each triangular patch  $\gamma \in \Gamma_{h/m}^{2 \rightarrow 1}$ ,
- $\int_{\Omega_h^\Gamma}^5 \cdot \, d\mathbf{x}$  denotes a composite quadrature rule that is exact for  $\bar{P}_h^5(\Omega_h^\Gamma)$ , i.e. this quadrature is exact for piecewise polynomials up to degree 5 on each tetrahedron  $T \in \Omega_h^\Gamma$ ,
- $E_{s, \Gamma_h^2}$  and  $\operatorname{div}_{\Gamma_h^2}$  are defined as their continuous analogues with  $\mathbf{n}_\Gamma$  in  $\mathbf{P}$  replaced with  $\mathbf{n}_{\Gamma_h^2}$ ,
- It is always the case that integrands use  $\mathbf{n}_{\Gamma_h^2} \neq \mathbf{n}_{\Gamma_{h/m}^{2 \rightarrow 1}}$ , and the actual domain of integration is  $\Gamma_{h/m}^{2 \rightarrow 1} \neq \Gamma_h^2$ ,
- $\mathbf{n}_{\Gamma_h^2}$  is defined in (14) and it is not a polynomial even locally, thus quadrature rules are never exact (although for  $\mathbf{P}_2 - P_1$  shape functions alone these quadratures are exact).

### 3.5 Using exact normals in integrands of $\int_{\Gamma_{h/m}^{2 \rightarrow 1}}$ (updated summary)

It was quite easy to update (16) such that the exact normals w.r.t. piecewise linear surface domain of integration are used. `spatch` (section 3.3) has a member function that gives **physical** normals to its triangles straightaway. Thus implementation of updated quadratures boiled down to constructing `GridFunction` object (described in section 3.2) out of these physical normals. Details of the implementation can be found in commit [dacc440](#).

Comments:

- It is also easy to extend this approach s.t.  $\Gamma_{h/m}^1 \neq \Gamma_{h/m}^{2 \rightarrow 1}$  is used (please see section 3.1 and then figures 5 and 6). There is no difference between  $\Gamma_{h/2}^{2 \rightarrow 1}$  and  $\Gamma_{h/2}^1$ . For  $m > 2$ , there is no difference between  $\Gamma_{h/m}^{2 \rightarrow 1}$  and  $\Gamma_{h/m}^1$  if  $\phi \in P^2$ . Right now  $\Gamma_{h/m}^{2 \rightarrow 1}$  is implemented.
- It is **not** that easy to use the exact normal w.r.t. piecewise linear surface domain of integration in volume integrals. Our guess is that it shall not be a problem (we can leave  $\mathbf{n}_{\Gamma_h^2}$  there),

- It is **not** easy to build  $I_h^n(\phi)$  for  $n > 2$ . It is **not** implemented in DROPS as for now.

As for now, the matrices in (1) can also be assembled as

$$\begin{aligned}
\langle \mathbf{A} \vec{\mathbf{u}}, \vec{\mathbf{v}} \rangle &= \int_{\Gamma_{h/m}^{2 \rightarrow 1}}^5 \left( E_{s, \Gamma_{h/m}^{2 \rightarrow 1}}(\mathbf{u}) : E_{s, \Gamma_{h/m}^{2 \rightarrow 1}}(\mathbf{v}) + \mathbf{u} \cdot \mathbf{v} + \tau (\mathbf{u} \cdot \mathbf{n}_{\Gamma_h^2}) (\mathbf{v} \cdot \mathbf{n}_{\Gamma_h^2}) \right) ds \\
&\quad + \rho_u \int_{\Omega_h^\Gamma}^5 \frac{\partial \mathbf{u}}{\partial \mathbf{n}_{\Gamma_h^2}} \cdot \frac{\partial \mathbf{v}}{\partial \mathbf{n}_{\Gamma_h^2}} d\mathbf{x}, \quad \mathbf{A} \in \mathbb{R}^{n_A \times n_A}, \\
\langle \mathbf{B} \vec{\mathbf{u}}, \vec{\mathbf{q}} \rangle &= - \int_{\Gamma_{h/m}^{2 \rightarrow 1}}^5 q \operatorname{div}_{\Gamma_{h/m}^{2 \rightarrow 1}} \mathbf{u} ds, \quad \mathbf{B} \in \mathbb{R}^{n_S \times n_A}, \\
\langle \mathbf{M}_0 \vec{\mathbf{p}}, \vec{\mathbf{q}} \rangle &= \int_{\Gamma_{h/m}^{2 \rightarrow 1}}^5 p q ds, \quad \mathbf{M}_0 \in \mathbb{R}^{n_S \times n_S}, \\
\langle \mathbf{C}_n \vec{\mathbf{p}}, \vec{\mathbf{q}} \rangle &= \rho_p \int_{\Omega_h^\Gamma}^5 \frac{\partial p}{\partial \mathbf{n}_{\Gamma_h^2}} \frac{\partial q}{\partial \mathbf{n}_{\Gamma_h^2}} d\mathbf{x}, \quad \mathbf{C}_n \in \mathbb{R}^{n_S \times n_S}, \\
\langle \mathbf{C}_{\text{full}} \vec{\mathbf{p}}, \vec{\mathbf{q}} \rangle &= \rho_p \int_{\Omega_h^\Gamma}^5 \nabla p \cdot \nabla q d\mathbf{x}, \quad \mathbf{C}_{\text{full}} \in \mathbb{R}^{n_S \times n_S},
\end{aligned} \tag{17}$$

Notations are as in (16). Note that the “ $\tau$ -term” uses  $\mathbf{n}_{\Gamma_h^2}$ . In order to switch between (16) and (17), one modifies JSON input file:

```

// No_Bnd_Condition.json
"Levelset": {
// ...
"NumbOfVirtualSubEdges" : 2,
"UseExactNormals"       : "yes",
// ...
}

```

Here 2 corresponds to  $m = 2$ , and “yes” corresponds to (17).



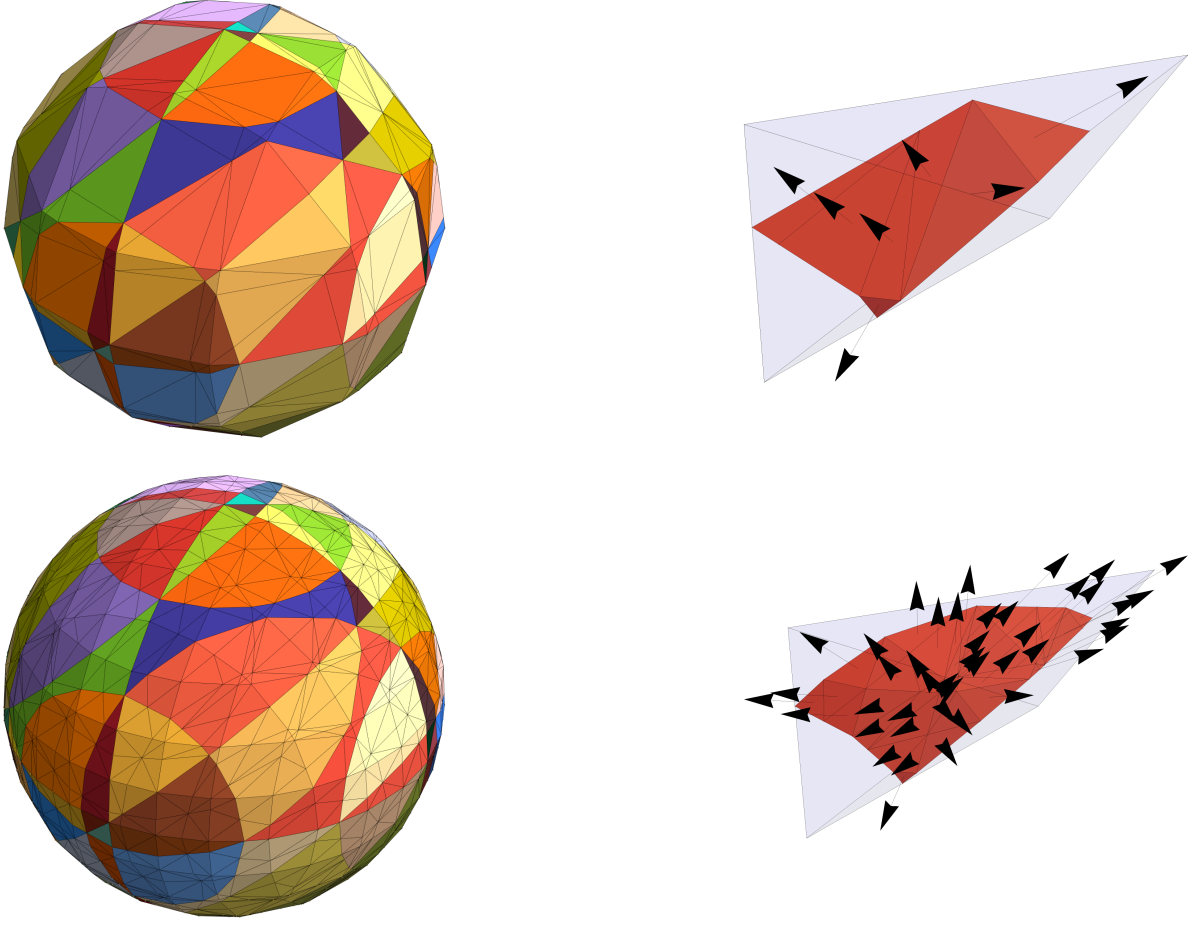


Figure 5:  $\Gamma = \Gamma_{\text{sph}}$ ,  $\phi(\mathbf{x}) = \|\mathbf{x}\|^2 - 1$ ,  $h = 8.33 \times 10^{-1}$ . Top-left:  $\Gamma_{h/2}^{2 \rightarrow 1} = \Gamma_{h/2}^1$  (different color corresponds to a different **spatch**  $\gamma \in \Gamma_{h/2}^{2 \rightarrow 1}$  as described in section 3.3). Top-right: a patch  $\gamma \in \Gamma_{h/2}^{2 \rightarrow 1}$  and its normals. Bottom-left and bottom-right: same for  $\Gamma_{h/4}^{2 \rightarrow 1} = \Gamma_{h/4}^1$ . **Note that since  $\phi \in P^2$ , we have that  $\Gamma_{h/m}^{2 \rightarrow 1} = \Gamma_{h/m}^1 \rightarrow \Gamma$  as  $m \rightarrow \infty$  independent of  $h$**

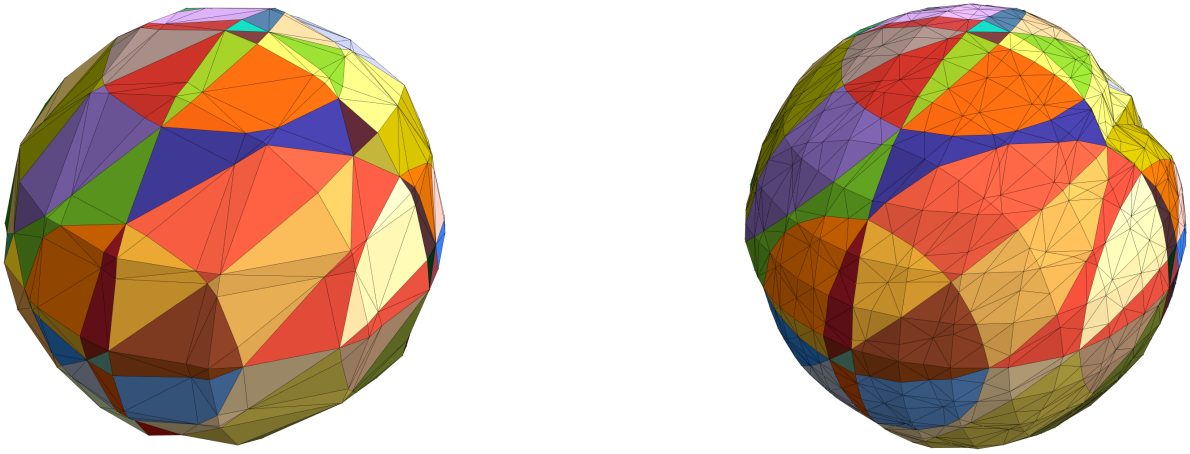


Figure 6:  $\Gamma = \Gamma_{\text{sph}}$ ,  $\phi(\mathbf{x}) = \|\mathbf{x}\|^{1/2} - 1$ ,  $h = 8.33 \times 10^{-1}$ . Left:  $\Gamma_{h/2}^{2 \rightarrow 1} = \Gamma_{h/2}^1$  (different color corresponds to a different **spatch**  $\gamma \in \Gamma_{h/2}^{2 \rightarrow 1}$  as described in section 3.3). Right: same for  $\Gamma_{h/4}^{2 \rightarrow 1} \neq \Gamma_{h/4}^1$ . **Note that since  $\phi \notin \bar{P}_h^2$ , we have that  $\Gamma_{h/m}^{2 \rightarrow 1} \neq \Gamma_{h/m}^1$  for  $m > 2$ , and  $\Gamma_{h/m}^{2 \rightarrow 1} \rightarrow \Gamma_h^2 \neq \Gamma$  as  $m \rightarrow \infty$  for fixed  $h$**

### 3.6 Quadrature rules for the error computation

When we first tried to test convergence for (17) in section 2, we noticed that the  $\mathbb{H}^1(\Gamma)$ -error of the velocity decays much slower than expected, whereas its  $\mathbb{L}^2(\Gamma)$ -error behaves as expected. Note that  $\mathbb{H}^1(\Gamma)$ -error (for e.g.  $\mathbf{P}_2-P_1$  FE) can be computed as  $\langle \mathbf{w}, \mathbf{A}_s \mathbf{w} \rangle^{1/2}$ ,  $\mathbf{w} :=$  vector of d.o.f. corresponding to  $\mathbf{P}_h^2$  interpolant  $I_h^2(\mathbf{u}) - \mathbf{u}_h$ ,  $\mathbf{A}_s :=$  matrix corresponding to the first term of  $\mathbf{A}$  in (17). Thus the errors are approximated as

$$\begin{aligned}\|\mathbf{u} - \mathbf{u}_h\|_{\mathbb{H}^1(\Gamma)} &= \|I_h^k(\mathbf{u}) - \mathbf{u}_h\|_{\mathbb{H}^1(\Gamma_{h/m}^{2 \rightarrow 1})} + O(h^k), \\ \|\mathbf{u} - \mathbf{u}_h\|_{\mathbb{L}^2(\Gamma)} &= \|I_h^k(\mathbf{u}) - \mathbf{u}_h\|_{\mathbb{L}^2(\Gamma_{h/m}^{2 \rightarrow 1})} + O(h^{k+1}), \\ \|p - p_h\|_{\mathbb{L}^2(\Gamma)} &= \|I_h^1(p) - p_h\|_{\mathbb{L}^2(\Gamma_{h/m}^{2 \rightarrow 1})} + O(h^2)\end{aligned}$$

for large enough  $m$ . Here  $k = 1$  for  $\mathbf{P}_1-P_1$  FEM and  $k = 2$  for  $\mathbf{P}_2-P_1$ .

**Interestingly enough**, DROPS implementation did not use the assembled matrices to compute errors (and normals that are *different* from the ones in  $\mathbf{A}_s$  were used). We corrected it in commit [68443b0](#):

```
// surfnavierstokes.cpp
// ...
VectorCL vSolMinusV = vSol.Data - v.Data, pSolMinusP = pSol.Data - p.Data;
auto velL2          = sqrt(dot(v.Data, M.Data * v.Data));
auto velNormalL2    = sqrt(dot(v.Data, S.Data * v.Data));
auto velH1err       = sqrt(dot(vSolMinusV, A.Data * vSolMinusV));
auto velL2err       = sqrt(dot(vSolMinusV, M.Data * vSolMinusV));
auto preL2          = sqrt(dot(p.Data, Schur.Data * p.Data));
auto preL2err       = sqrt(dot(pSolMinusP, Schur.Data * pSolMinusP));
// ...
```

## References

- [1] M. Olshanskii, A. Quaini, A. Reusken, and V. Yushutin. A finite element method for the surface stokes problem. *SIAM Journal on Scientific Computing*, 40(4):A2492–A2518, 2018.